Available online at www.sciencedirect.com
SCIENCE DIRECT
Journal of Power Sources 146 (2005) 640–644
JOURNAL OF POWER SOURCES
www.elsevier.com/locate/jpowsour

Investigation on lithium de-intercalation mechanism for $Li_{1-y}Ni_{1/3}Mn_{1/3}Co_{1/3}O_2$

Hironori Kobayashi [a,*], Yoshinori Arachi [b], Shuichi Emura [c], Hiroyuki Kageyama [a], Kuniaki Tatsumi [a], Takashi Kamiyama [d]

[a] *Research Institute for Ubiquitous Energy Devices, National Institute of Advanced Industrial Science and Technology (AIST), Ikeda, Osaka 563-8577, Japan*
[b] *Unit of Chemistry, Faculty of Engineering, Kansai University, Suita, Osaka 564-8680, Japan*
[c] *Institute of Scientific and Industrial Research (ISIR), Osaka University, Ibaraki, Osaka 567-0047, Japan*
[d] *Institute of Materials Structure Science, High Energy Accelerator Research Organization (KEK), Tsukuba, Ibaraki 305-0801, Japan*

Available online 1 June 2005

Abstract

$Li_{1-y}Ni_{1/3}Mn_{1/3}Co_{1/3}O_2$ ($y = 0$–0.7) was characterized using neutron diffraction and X-ray absorption fine structure (XAFS) measurements. $LiNi_{1/3}Mn_{1/3}Co_{1/3}O_2$ adopted the α-$NaFeO_2$ structure and was demonstrated that the chemical formula can be expressed as $[Li_{0.97}Ni_{0.03}]_{3a}[Li_{0.03}Ni_{0.30}Mn_{0.33}Co_{0.33}]_{3b}O_2$. The Li/$Li_{1-y}Ni_{1/3}Mn_{1/3}Co_{1/3}O_2$ cell showed a discharge capacity of 160 mAh g^{-1} in the voltage range 4.6–2.5 V. The Ni K and $L_{II,III}$-edge X-ray absorption near edge structure (XANES) results clarified the contribution of the Ni ion to charge compensation up to $y = 0.7$ and the rehybridization of the Ni 3d orbital with O 2p orbital above $y = 0.5$. The Co K-edge extended X-ray absorption fine structure (EXAFS) results clarified that the Co─O bond lengths decreased up to $y = 0.7$ with Li de-intercalation, while the Mn K-edge EXAFS results indicated that the Mn─O bond lengths showed essentially no change over the whole composition range. These results supported that the Li de-intercalation from $LiNi_{1/3}Mn_{1/3}Co_{1/3}O_2$ proceeded mainly by the valence state change of Ni and Co ions over the whole composition range. The combination of XAFS analysis using hard and soft X-ray data is a powerful method in clarifying the mechanism of the Li de-intercalation process in this system.

Keywords: Li secondary battery; Layered oxides; Neutron diffraction measurement; XAFS measurement

1. Introduction

Recent reports have shown that the layered oxides $LiNi_{0.5}Mn_{0.5}O_2$ and $LiCo_{1/3}Ni_{1/3}Mn_{1/3}O_2$ are promising cathode materials for lithium secondary batteries [1–6]. Both $LiNi_{0.5}Mn_{0.5}O_2$ and $LiCo_{1/3}Ni_{1/3}Mn_{1/3}O_2$ adopt the rhombohedral structure of $LiCoO_2$ and $LiNiO_2$ and possess reversible capacities of 150 mAh g^{-1} in the voltage range 2.5–4.3 V and of 200 mAh g^{-1} in the voltage range 2.5–4.6 V, respectively. They show the superior characteristics of larger capacities compared to $LiMn_2O_4$ and better thermal stability compared to $LiNiO_2$. Many researchers have concentrated their efforts on synthesizing related doped materials in order to improve the cycle life and thermal stability until now [7–12].

We have reported on the changes in the structure and physical properties of various compositions in the solid solutions $LiNi_{1-x}Mn_xO_2$, $Li_{1-y}Ni_{0.5}Mn_{0.5}O_2$, and $Li_{1-y}Ni_{0.5}Mn_{0.4}Ti_{0.1}O_2$ using a combination of synchrotron XRD analysis, neutron diffraction (ND) analysis, maximum entropy method (MEM), and magnetic measurements as effective tools for characterizing these systems better [5,6,13–15]. $LiNi_{1-x}Mn_xO_2$ can be represented as $Li(Ni^{2+}{}_xNi^{3+}{}_{1-2x}Mn^{4+}{}_x)O_2$ and the chemical formula of $LiNi_{0.5}Mn_{0.5}O_2$ can be expressed as $[Li_{0.91}Ni_{0.09}]_{3a}[Li_{0.09}Mn_{0.5}Ni_{0.41}]_{3b}O_2$ [5]. In addition, we clarified the structural change in $LiNi_{0.5}Mn_{0.5}O_2$ during Li de-intercalation process, demon-

* Corresponding author. Tel.: +81 72 751 9649; fax: +81 72 751 9609.
E-mail address: hironori-kobayashi@aist.go.jp (H. Kobayashi).

0378-7753/$ – see front matter © 2005 Elsevier B.V. All rights reserved.
doi:10.1016/j.jpowsour.2005.03.081

strating that it proceeds via a single-phase reaction. A monoclinic phase was clearly observed at $y = 0.5$ in $Li_{1-y}Ni_{0.5}Mn_{0.5}O_2$ [6] and the chemical formula of this phase can be represented as $[Ni_{0.0815}]_{2a}\{Li_{0.5}Ni_{0.0115}\}_{4i}[Mn_{0.5}Ni_{0.41}\square_{0.093}]_{2d}O_2$ [13]. Detailed information on the phase transition of $Li_{1-y}Ni_{0.5}Mn_{0.5}O_2$ is very important in order to improve the electrochemical properties of not only this solid solution but also of related materials.

In the present study, we synthesized $Li_{1-y}Co_{1/3}Ni_{1/3}Mn_{1/3}O_2$ ($y = 0$–0.7) and investigated the electrical and local structural changes of $Li_{1-y}Co_{1/3}Ni_{1/3}Mn_{1/3}O_2$ systematically using a combination of ND and XAFS (hard and soft XAFS) measurements. We discussed the mechanism of the Li de-intercalation process in this system.

2. Experimental

$LiNi_{1/3}Mn_{1/3}Co_{1/3}O_2$ was prepared using appropriate molar ratios of $LiOH{\cdot}H_2O$, $Ni(CH_3COO)_2{\cdot}4H_2O$, $Mn(CH_3COO)_2{\cdot}4H_2O$, and $Co(CH_3COO)_2{\cdot}4H_2O$. The mixtures of $M(CH_3COO)_2{\cdot}4H_2O$ (M = Ni, Mn, Co) were calcined in air at 973 K for 12 h to convert the metal oxalates to oxides. The resulting oxides were weighed along with $LiOH{\cdot}H_2O$, mixed, pelletized, and fired in air at 1273 K for 24 h. $Li_{1-y}Ni_{1/3}Mn_{1/3}Co_{1/3}O_2$ ($y = 0.1$–0.7) was prepared electrochemically using a coin-type cell comprised of Li/1M $LiPF_6$ in EC:DEC (=1:1) solution/$LiNi_{1/3}Mn_{1/3}Co_{1/3}O_2$, with a BTS2004 (Nagano Co. Ltd.) apparatus. The cathode consisted of a mixture having weight composition ratio 86($LiNi_{1/3}Mn_{1/3}Co_{1/3}O_2$):6(acetylene black):8(PVDF binder).

ND data were collected at room temperature on the neutron powder diffractometer, HERMES, at the Tokai Establishment of the Japan Atomic Energy Research Institute (JAERI). The wavelength of the incident neutrons was fixed at 1.82035 Å. The structural parameters were refined by Rietveld analysis using the computer program RIETAN2000 [16] for the ND data.

The Ni, Mn, and Co K-edge X-ray absorption near edge structure (XAFS) spectra of the samples were measured on the BL7C of the Photon Factory at the National Laboratory for High Energy Physics (KEK-PF) (Proposal No. 2001G123). The measurements were performed in transmission mode, the incident X-rays were monochromatized with a Si(1 1 1) crystal and a detuning method was used for the suppression of higher harmonics in Mn absorption measurements. Extended X-ray absorption fine structure (EXAFS) data were analyzed using Rigaku REX2000 software. Backgrounds were subtracted using an extrapolated Victoreen-plus-constant type function and the EXAFS oscillations $\chi(k)$ were extracted using cubic spline baseline functions. Fourier transforms were performed on the normalized $\chi(k)$ with k^3 weighting of a Hanning window in the region $k = 2.5$–15.0 for Mn K-edge and $k = 2.5$–12.0 for Co K-edge.

The Ni, Mn, and Co $L_{II,III}$-edge X-ray absorption near edge structure (XANES) spectra of the samples were measured on the BL1A of the UVSOR Facility at the Institute for Molecular Science (Proposal No. 16-556). The measurements were performed in total electron yield mode, the incident X-rays were monochromatized with a β-Al_2O_3 crystal.

3. Results and discussion

3.1. Synthesis and characterization

$LiNi_{1/3}Mn_{1/3}Co_{1/3}O_2$ was synthesized in air at 1273 K for 24 h. The Li/Ni/Mn/Co molar ratio of this phase was determined to be 1.00:0.34:0.33:0.33 by ICP emission spectrometry. The composition was thus confirmed to be $LiNi_{1/3}Mn_{1/3}Co_{1/3}O_2$. We reported that the 3a site is occupied by a small proportion of Ni ions in $LiNi_{0.5}Mn_{0.5}O_2$ using ND measurements [5]; In this case, Ni can be distinguished from Mn because of the difference in coherent scattering lengths ($b_c(Ni) = 1.034 \times 10^{-12}$ cm and $b_c(Mn) = -0.373 \times 10^{-12}$ cm).

The structure of $LiNi_{1/3}Mn_{1/3}Co_{1/3}O_2$ was refined using neutron diffraction data, the initial model being that of $LiNi_{0.5}Mn_{0.5}O_2$ [5], with space group $R\bar{3}m$ and atomic positions Li1/Ni1 at 3a(0, 0, 0), Li2/Ni2/Mn/Co at 3b(0, 0, 1/2), and O at 6c(0, 0, z) where $z \sim 0.25$. On the basis of this structural model, we attempted to accurately determine both the distribution of the cations on the 3a and 3b sites and the thermal factors using ND data. The occupation parameters of Mn and Co at the 3b site were fixed and that of Ni2 at the 3b site was refined. The total occupancies of both the 3b sites containing Li2/Ni2/Mn/Co and the 3a sites containing Li1/Ni1 were constrained to be unity [Li2(g) + Ni2(g) + Mn(g) + Co(g) = 1 and Li1(g) + Ni1(g) = 1]. Further constraints were introduced such that the sum of the Li occupancies over the two sites was constrained to be unity [Li1(g) + Li2(g) = 1] and the sum of the Ni occupancies was that of the value corresponding to the composition [Ni1(g) + Ni2(g) + Mn(g) + Co(g) = 1]. We can confirm that our refined structural model showed good fitting with low R value. Fig. 1 shows the observed, calculated and difference diffraction profiles for the ND Rietveld refinement of the host material $LiNi_{1/3}Mn_{1/3}Co_{1/3}O_2$, and the structural parameters are summarized in Table 1. These results imply that the chemical formula of $LiNi_{1/3}Mn_{1/3}Co_{1/3}O_2$ can be represented as $[Li_{0.97}Ni_{0.03}]_{3a}[Li_{0.03}Ni_{0.30}Mn_{0.33}Co_{0.33}]_{3b}O_2$.

3.2. XANES measurements

$Li_{1-y}Ni_{1/3}Mn_{1/3}Co_{1/3}O_2$ ($y = 0.1$–0.7) was synthesized electrochemically. Fig. 2 shows the first charge and discharge curves of $LiNi_{1/3}Mn_{1/3}Co_{1/3}O_2$. The Li/$LiNi_{1/3}Mn_{1/3}Co_{1/3}O_2$ cell had a discharge capacity of 160 mAh g^{-1} in the voltage range 4.6–2.5 V. Fig. 3 shows

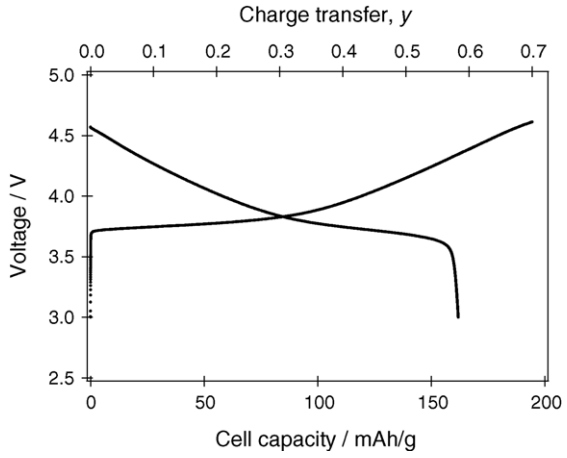

Fig. 1. First charge and discharge curves of the Li/$LiNi_{1/3}Mn_{1/3}Co_{1/3}O_2$ cell with a current density of 0.2 mA cm^{-2}.

Table 1
Structural parameters for $LiNi_{1/3}Mn_{1/3}Co_{1/3}O_2$ determined using the neutron data

Atom	Site	g	x	y	z	B (Å^2)
Ni	3a	0.0337	0	0	0	0.40(13)
Li	3a	0.9663	0	0	0	=B(Ni)
Ni2	3b	0.2996(17)	0	0	1/2	0.02(8)
Li2	3b	0.0337	0	0	1/2	=B(Ni2)
Mn	3b	0.3333	0	0	1/2	=B(Ni2)
Co	3b	0.3333	0	0	1/2	=B(Ni2)
O	6c	1	0	0	0.24126(8)	0.77(4)

$a = 2.8598(17)$ Å, $c = 14.225(6)$ Å, $R_{wp} = 5.57\%$, $R_e = 3.74\%$, $R_I = 3.24\%$, $R_F = 1.84\%$.

the Ni K-edge XANES spectrum. The Ni K-edge XANES spectrum corresponds to a valence state of Ni^{2+} at $y = 0$ and displays a continuously shift to higher photon energy up to $y = 0.6$, indicating a change in the valence state first to Ni^{3+} and then to Ni^{4+} on de-lithiation. There is a little shift in energy between $y = 0.6$ and 0.7. On the other hand, the Mn and Co K-edge XANES spectra correspond to valence states of essentially Mn^{4+} and Co^{3+} respectively at $y = 0$,

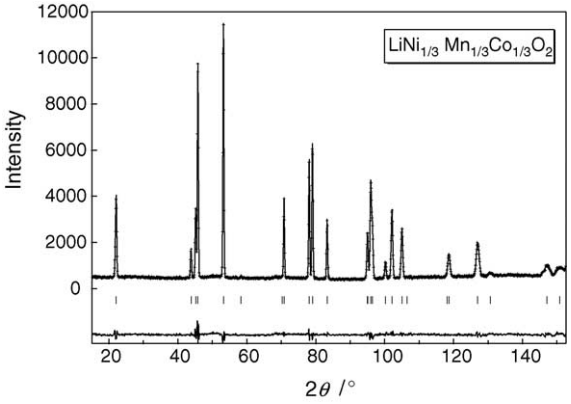

Fig. 2. Observed, calculated and difference diffraction profiles of $LiNi_{1/3}Mn_{1/3}Co_{1/3}O_2$ for Rietveld refinement using ND data.

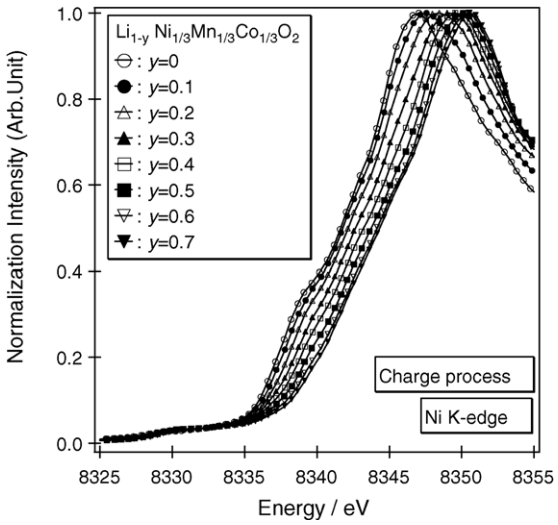

Fig. 3. Ni K-edge XANES spectra for $Li_{1-y}Ni_{1/3}Mn_{1/3}Co_{1/3}O_2$ ($y = 0$–0.7).

and show little deviation from the valence states of Mn^{4+} and Co^{3+} up to $y = 0.7$. Fig. 4 shows the Ni $L_{II,III}$-edge XANES spectrum. The Ni $L_{II,III}$-edge XANES spectrum at $y = 0$ is similar to that of NiO with a valence state of Ni^{2+}. The Ni L_{II}-edge XANES spectrum shows a continuously shift up to $y = 0.7$, while the Ni L_{III}-edge XANES spectrum shows the appearance of a shoulder peak at ~855 eV clearly above $y = 0.5$, indicating the rehybridization of the Ni 3d orbital with O 2p orbital. On the other hand, the Mn and Co $L_{II,III}$-edge XANES spectra show essentially little change over the whole composition range.

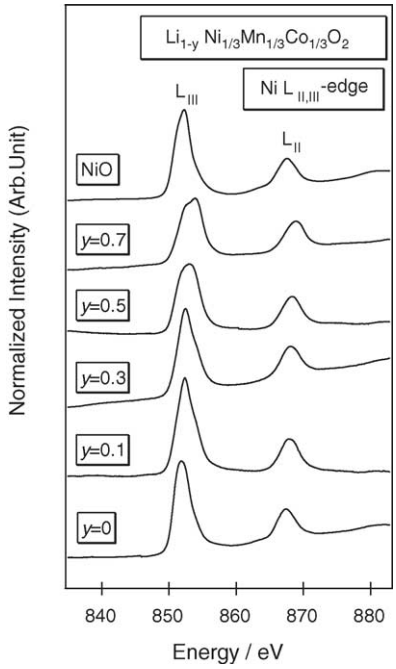

Fig. 4. Ni $L_{II,III}$-edge XANES spectra for $Li_{1-y}Ni_{1/3}Mn_{1/3}Co_{1/3}O_2$ ($y = 0$–0.7).

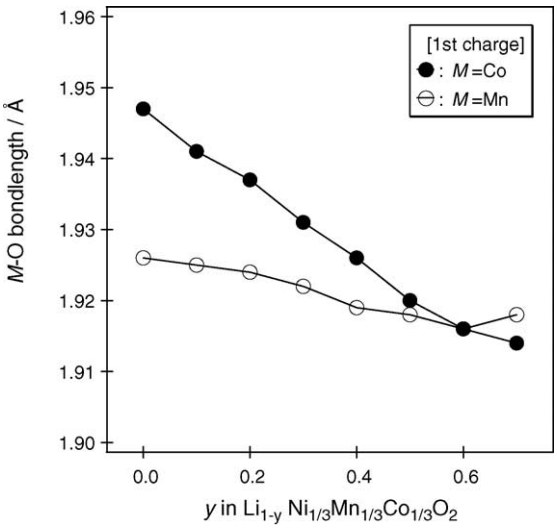

Fig. 5. Composition dependence of the M—O (M = Mn and Co) bond length.

3.3. Local structure

The changes in local structure around M (M = Mn and Co) cations were also investigated, using the M K-edge EXAFS measurements. In our study scattering from the Li atoms has been neglected since the photoelectron backscattering amplitude from Li is very weak. Curve fitting was carried out using one shell model in the filtered range $R = 1.0$–2.0 Å for M–O (M = Mn and Co). The coordination number was fixed at 6. Fig. 5 shows the composition dependence of the M–O (M = Mn and Co) bond length. The increase of Co^{4+} content on de-lithiation is clearly illustrated in Fig. 5 where the Co–O bond length becomes smaller from 1.947 to 1.914 Å up to $y = 0.7$. On the other hand, the Mn–O bond length shows essentially no deviation from the values of 1.926–1.916 Å over the whole composition ranges. Thus, EXAFS analysis has demonstrated that the extraction of Li ions from $LiNi1_{/3}Mn_{1/3}Co_{1/3}O_2$ proceeded partially by a valence state change from Co^{3+} to Co^{4+} up to $y = 0.7$.

3.4. Discussion

We have reported that the chemical formula of $LiNi_{0.5}Mn_{0.5}O_2$ can be expressed as $[Li_{0.91}Ni_{0.09}]_{3a}[Li_{0.09}Mn_{0.5}Ni_{0.41}]_{3b}O_2$ [5]. In this study, we clarified that the chemical formula of $LiNi_{1/3}Mn_{1/3}Co_{1/3}O_2$ can be represented as $[Li_{0.97}Ni_{0.03}]_{3a}[Li_{0.03}Ni_{0.30}Mn_{0.33}Co_{0.33}]_{3b}O_2$. These results imply that the Co-doping to $LiNi_{0.5}Mn_{0.5}O_2$ is effective way to suppress the disordering of Li and Ni ions between the 3a and the 3b sites.

Several researchers have reported on Li de-intercalation mechanism in $LiNi_{0.5}Mn_{0.5}O_2$-related materials from the perspective of the electronic structure. One of the authors (YA) reported that the extraction of Li from $LiNi_{0.5}Mn_{0.5}O_2$ proceeded in association with oxidation of Ni^{2+} to Ni^{3+}, not oxidation of Mn, from the Ni and Mn K-edge XAFS spectroscopy [6]. Sun et al. reported that the oxygen ions are responsible for charge compensation during the charge–discharge process in $Li_{1-y}[Li_{0.15}Ni_{0.275-x}Mg_xMn_{0.575}]O_2$ ($x = 0$ and 0.04) and $Li_{1-y}Ni_{0.5}Mn_{0.5}O_2$ using the O K-edge XANES spectroscopy [9]. Yoon et al. reported that the holes compensating Li ion de-intercalation are located in O 2p states as well as Ni 3d state at higher states of charge in $Li_{1-y}Ni_{0.5}Mn_{0.5}O_2$ using the O K-edge XANES spectroscopy in the fluorescence yield mode [17].

In this study, the Ni K and $L_{II,III}$-edge XANES results indicated the contribution of the Ni ion to charge compensation up to $y = 0.7$ in $Li_{1-y}Ni_{1/3}Mn_{1/3}Co_{1/3}O_2$. The Co K-edge EXAFS results indicated that the change in valence state from Co^{3+} to Co^{4+} as y increased was clearly detected by a decrease of the Co–O distances. These results supported that the Li de-intercalation proceeded mainly by the valence state change of Ni and Co ions over the whole composition range. The combination of XAFS analysis using hard and soft X-ray data is a powerful method in clarifying the mechanism of the Li de-intercalation process in this system.

4. Conclusion

Structural analysis using ND data demonstrated that the chemical composition of $LiNi_{1/3}Mn_{1/3}Co_{1/3}O_2$ can be expressed as $[Li_{0.97}Ni_{0.03}]_{3a}[Li_{0.03}Ni_{0.30}Mn_{0.33}Co_{0.33}]_{3b}O_2$ and that Co-doping to $LiNi_{0.5}Mn_{0.5}O_2$ is effective way to suppress the disordering of Li and Ni ions between the 3a and the 3b sites. The $Li/LiNi_{1/3}Mn_{1/3}Co_{1/3}O_2$ cell showed a discharge capacity of 160 mAh g^{-1} in the voltage range 4.6–2.5 V. The XAFS analysis using both hard and soft X-ray data clarified that the extraction of lithium from $Li/LiNi_{1/3}Mn_{1/3}Co_{1/3}O_2$ proceeded mainly by the oxidation of Ni and Co ions.

References

[1] T. Ohzuku, Y. Makimura, Chem. Lett. (2001) 744–745.
[2] Z. Lu, D.D. MacNeil, J.R. Dahn, Electrochem. Solid State Lett. 4 (2001) A191–A194.
[3] L. Zhang, H. Noguchi, M. Yoshio, J. Power Sources 110 (2002) 57–64.
[4] N. Yabuuchi, T. Ohzuku, J. Power Sources 119–121 (2003) 171–174.
[5] H. Kobayashi, H. Sakaebe, H. Kageyama, K. Tatsumi, Y. Arachi, T. Kamiyama, J. Mater. Chem. 13 (2003) 590–595.
[6] Y. Arachi, H. Kobayashi, S. Emura, Y. Nakata, M. Tanaka, T. Asai, Chem. Lett. 32 (2003) 60–61.
[7] C.S. Johnson, J.S. Kim, A.J. Kropf, A.J. Kahaian, J.T. Vaughey, M.M. Thackeray, Electrochem. Commun. 4 (2002) 492–498.
[8] Z. Lu, J.R. Dahn, J. Electrochem. Soc. 149 (2002) A815–A822.
[9] Y.K. Sun, M.G. Kim, S.-H. Kang, K. Amine, J. Mater. Chem. 13 (2003) 319–322.
[10] D.D. MacNeil, Z. Lu, J.R. Dahn, J. Electrochem. Soc. 149 (2002) A1332–A1336.
[11] S.-H. Kang, J. Kim, M.E. Stoll, D. Abraham, Y.K. Sun, K. Amine, J. Power Sources 112 (2002) 41–148.

[12] S.H. Park, Y.K. Sun, J. Power Sources 119–121 (2003) 161–165.
[13] H. Kobayashi, Y. Arachi, H. Kageyama, K. Tatsumi, J. Mater. Chem. 14 (2004) 40–42.
[14] H. Kobayashi, Y. Arachi, H. Kageyama, H. Sakaebe, K. Tatsumi, D. Mori, R. Kanno, T. Kamiyama, Solid State Ionics 175 (2004) 221–224.
[15] Y. Arachi, H. Kobayashi, S. Emura, Y. Nakata, M. Tanaka, T. Asai, H. Sakaebe, K. Tatsumi, H. Kageyama, Solid State Ionics 176 (2005) 895–903.
[16] F. Izumi, T. Ikeda, Mater. Sci. Forum 321–324 (2000) 198.
[17] W.-S. Yoon, M. Balasubramanian, X-Q. Yang, Z. Fu, D.A. Fischer, J. McBreen, J. Electrochem. Soc. 151 (2004) 246–251.